Published in final edited form as:
Biomaterials. 2012 October ; 33(30): 7478–7488. doi:10.1016/j.biomaterials.2012.06.097.

Iterative design of peptide-based hydrogels and the effect of network electrostatics on primary chondrocyte behavior

Chomdao Sinthuvanich[a,b], **Lisa A. Haines-Butterick**[b], **Katelyn J. Nagy**[a,b], and **Joel P. Schneider**[a,*]

[a]Chemical Biology Laboratory, National Cancer Institute, Frederick National Laboratory for Cancer Research, Frederick, MD 21702, USA

[b]Department of Chemistry and Biochemistry, University of Delaware, Newark, DE 19716, USA

Abstract

Iterative peptide design was used to generate two peptide-based hydrogels to study the effect of network electrostatics on primary chondrocyte behavior. MAX8 and HLT2 peptides have formal charge states of +7 and +5 per monomer, respectively. These peptides undergo triggered folding and self-assembly to afford hydrogel networks having similar rheological behavior and local network morphologies, yet different electrostatic character. Each gel can be used to directly encapsulate and syringe-deliver cells. The influence of network electrostatics on cell viability after encapsulation and delivery, extracellular matrix deposition, gene expression, and the bulk mechanical properties of the gel-cell constructs as a function of culture time was assessed. The less electropositive HLT2 gel provides a microenvironment more conducive to chondrocyte encapsulation, delivery, and phenotype maintenance. Cell viability was higher for this gel and although a moderate number of cells dedifferentiated to a fibroblast-like phenotype, many retained their chondrocytic behavior. As a result, gel-cell constructs prepared with HLT2, cultured under static *in vitro* conditions, contained more GAG and type II collagen resulting in mechanically superior constructs. Chondrocytes delivered in the more electropositive MAX8 gel experienced a greater degree of cell death during encapsulation and delivery and the remaining viable cells were less prone to maintain their phenotype. As a result, MAX8 gel-cell constructs had fewer cells, of which a limited number were capable of laying down cartilage-specific ECM.

Keywords

Peptide; Hydrogel; Cell delivery; Self-assembly; Chondrocyte; Tissue engineering

1. Introduction

Cartilage is an avascular tissue essential for joint function. It provides a smooth and low-friction surface that cushions and protects the underlining bone from compressive loads and shear forces. Due to its avasculature nature, injured cartilage has a limited capacity to heal. Several clinical procedures have been developed to treat cartilage injuries such as arthroscopic debridement, marrow stimulation and osteochondral autografts [1, 2]. In addition, cell-based therapies are being explored to regenerate native-like cartilage. For example, in Autologous Chondrocyte Implantation (ACI), chondrocytes are introduced to a

*Corresponding author. Joel.Schneider@nih.gov, schneiderjp@mail.nih.gov (J.P. Schneider).

Appendix A. Supplementary material

Supplementary material associated with this article can be found, in the online version, at http://dx.doi.org/10.1016/j.biomaterials.2012.06.097.

defect site as a cellular suspension in media and a periosteal flap is used to confine the cells [3, 4]. Alternatively, cells can be seeded onto a material scaffold and cultured *ex vivo* affording cartilage-like tissue constructs that can be subsequently implanted [5].

Injectable hydrogels are now being explored to deliver cells in a minimally invasive manner for tissue engineering and cytomedical therapy [6]. Most materials coined as 'injectable gels' are actually delivered as liquids that undergo sol–gel transitions either during delivery or *in situ* after delivery [6]. For these systems, cells are suspended in a liquid precursor, syringe-delivered and ultimately encapsulated in the gel after the sol–gel transition takes place. The rate at which the sol–gel transition takes place is critical. If the rate of gelation is too fast, the material clogs the delivery device and if it is too slow, the cell-containing liquid precursor leaks to neighboring tissue resulting in low retention of cells at the implant site. Although there are some elegant examples of materials having appropriate rates of gelation [7, 8], the design of injectable materials as cell delivery vehicles remains challenging. Not only must the material display proper rheological properties during delivery, but after the gel has formed, it's mechanical stiffness, which is known to influence cell phenotype, must be strictly defined [9]. In addition, the material's cytocompatibility and biocompatibility must be commensurate with cell type and the specific tissue to which the cells are being delivered.

Our lab is developing a hydrogel system that allows cells to be syringe-delivered while encapsulated in a solid-like gel, eliminating the need to rely on a sol–gel phase transition to take place during or after the delivery event [10, 11]. In this system, cells are encapsulated in a hydrogel network of self-assembled peptides, directly in a syringe. To encapsulate cells, unfolded peptides are first dissolved in aqueous buffer of low ionic strength. The subsequent addition of cell culture media triggers peptide folding into a β-hairpin conformation that undergoes rapid self-assembly, forming a fibrillar hydrogel network. When cells are present in the media, they are directly encapsulated in the hydrogel. The resulting solid-like gel-cell construct displays shear-thin/recovery mechanical properties. Thus, depressing the syringe plunger thins the gel, allowing it to flow through an attached narrow bore needle or catheter. On exiting the delivery device, the material immediately recovers its solid-like properties at the point of application. Pochan et al. have recently shown that during material-thinning through a narrow-bore capillary, the gel displays a flow profile characterized by a large central plug flow region and a very narrow shear zone close to the capillary wall. Thus, the vast majority of encapsulated cells are delivered in a plug of gel and do not experience significant shear rate during delivery [11]. The delivery mechanism afforded by these gels results in their acute retention at the implant site and allows the properties of the gel construct, such as its mechanical rigidity, microenvironment and cell density, to be strictly defined prior to cell delivery [10, 12–14].

Although controlling the mode of delivery is important in developing a new vehicle, others factors that influence cell fate during and after their delivery must be considered. Several studies have demonstrated that the electrostatic nature of a material can play an important role in regulating cell behavior. Electrostatic interactions between cells and substratum or surrounding network have been shown to affect cell viability [15], cell adhesion [16–18], proliferative capacity [19], and differentiation potential [20, 21]. Herein, an iterative peptide design approach is used to generate two hydrogels in order to determine if network electrostatics influences the ability of this class of peptide material to effectively encapsulate and deliver primary bovine chondrocytes, and to facilitate cartilage elaboration during tissue culture.

The two gels studied were prepared from MAX8 and HLT2, peptides that differ in their overall charge state at neutral pH, Table 1. MAX8, a previously published sequence, has an

overall charge state of +7 per monomer and self-assembled networks of this peptide are highly electropositive. A systematic, iterative design approach was used to generate HLT2. This peptide carries a +5 charge per monomer and forms a gel network that is significantly less electropositive. The design of HLT2 was challenging in that the peptide needed for this study had to be substantially different in its charge state and thus primary sequence, but form a gel of similar mechanical properties to those formed by MAX8. This ensures that any observable difference in the phenotype of cells cultured within each gel would be primarily due to the electrostatic nature of the network and not other differences, such as the stiffness of the gel, that are known to influence cell behavior [9]. As will be discussed, the electrostatic character of these gels significantly influences the behavior of encapsulated chondrocytes, with the less electropositive HLT2 gel providing a better microenvironment for cell encapsulation, delivery and *in vitro* cartilage elaboration.

2. Materials and methods

2.1. Materials

Fmoc-protected amino acids were purchased from Novabiochem. PL-rink amide resin was purchased from Polymer Laboratories. 1-H-benzotriazolium-1-[*bis*(di-methylamino) methylene]-5-chloro-hexafluorophosphate-(1-),3-oxide (HCTU) was obtained from Peptide International. Trifluoroacetic acid, triisopropylsilane and 30% hydrogen peroxide were obtained from Acros organics. Diethyl ether, xylene, 10% neutral buffered formalin and Permount mounting medium were purchased from Fisher Scientific. Heat-inactivated fetal bovine serum (FBS), penicillin/streptomycin solution, 0.25% trypsin/EDTA solution and phosphate buffer saline (PBS) were obtained from Hyclone Laboratory Inc. Collagenase II was purchased from Worthington Biochemical Co. Dulbecco's Modified Eagle's Medium supplemented with 25 mM HEPES (DMEM/HEPES), live-dead cytotoxicity/viability kit, CellTracker™ green CMFDA and TRIZol were purchased from Invitrogen. Power SYBR Green PCR Mastermix, random hexamer and RNase inhibitor were obtained from Applied Biosystems. Unless otherwise stated, all other reagents were purchased from Sigma Aldrich.

2.2. Peptide synthesis and purification

Peptides were synthesized on PL-rink amide resin using an automated ABI 433A peptide synthesizer (Applied Biosystems, CA). Synthesis was carried out via solid-phase Fmoc chemistry with HCTU activation. Dried resin-bound peptides were cleaved from the resin and side chain deprotected by a trifluoroacetic acid: triiso-propylsilane: deionized water (95:2.5:2.5) cocktail for 2 h under argon atmosphere. Crude peptides were precipitated using cold diethyl ether and then lyophilized. Reverse-phase-HPLC on semi-preparative Vydac C18 column was employed to purify the peptides. HPLC solvents consisted of Solvent A (0.1% TFA in water) and solvent B (0.1% TFA in 9:1 acetonitrile: water). Analytical HPLC and electrospray ionization (positive mode) mass spectrometry was performed to confirm the purity of the peptides. Lyophilized peptides were directly used for characterization and cell encapsulation with the exception of MAX8, which was dissolved in distilled water (1 mg/mL) and re-lyophilized twice before use.

2.3. Oscillatory rheology

Rheology experiments were performed on an AR-G2 rheometer (TA Instruments, DE) equipped with a 25-mm stainless steel parallel plate geometry with a 0.5 mm gap height. To investigate the rheological properties of the hydrogels at physiological condition, a 0.5 wt% peptide solution was prepared by first dissolving a 1 wt% stock of lyophilized peptide in a pH 7.4 buffer (25 mM HEPES). An equal volume of HEPES-supplemented DMEM (pre-incubated in CO_2) was subsequently added to peptide solution to initiate hydrogelation. 300 μL of resultant solution was immediately transferred to the rheometer plate equilibrated at

20 °C. A temperature ramp from 20 °C to 37 °C at a rate of 0.5 °C/s was then performed followed by an hour dynamic time sweep to monitor the evolution of the storage (G′) and loss (G″) moduli at an angular frequency of 6 rad/s and 0.2% strain. Oil was placed around the sample and on the plate to prevent evaporation.

To mimic syringe delivery, a similar procedure was followed to form the hydrogel. Here, after the temperature was ramped to 37 °C, the hydrogel was allowed to form for only 10 min at 6 rad/s and 0.2% strain. After which, 1000% strain was applied for 30 s at 1000% to disrupt the material. Subsequently, the ability of the hydrogel to reheal was monitored by measuring the recovery of G′ at 6 rad/s and 0.2% strain for additional 10 min.

2.4. Chondrocyte isolation

Knee joints of 24–30 month-old bovines were obtained on the day of slaughter. Cartilage was cut from the femoral condyles and minced into small pieces using a razor blade under sterile condition. Cartilage digestion was then carried out using a solution of 0.1% pronase in chondrogenic media at 37 °C, 5% CO_2 for 1 h. Chondrogenic media consists of Dulbecco's Modified Eagle's Medium (DMEM), 10% heat-inactivated FBS, 4 mM L-glutamine, 0.4 mM L-proline, 0.25 mM ascorbic acid phosphate magnesium salt N-hydrate, 0.1 mM non-essential amino acids, 100 U/mL penicillin, 100 U/mL streptomycin and 50 μg/mL gentamicin. The digestion in a solution of pronase was followed by digestion in a solution of 0.1% collagenase II in chondrogenic media for an additional 14–16 h at 37 °C 5% CO_2. The resulting cell suspension was then passed through two consecutive cell strainers, 100 and 70 μm respectively, and centrifuged at 2000 rpm for 15 min. The resulting chondrocytes were washed twice in PBS containing 2× penicillin/streptomycin and centrifuged again. The final pellet was resuspended in HEPES-supplemented DMEM at a density of 40×10^6 cells/mL and directly used for the cell studies unless stated otherwise. Viability of the cells after isolation was determined by trypan blue exclusion to be about 95% viability or higher.

2.5. Chondrocyte encapsulation and syringe delivery

To demonstrate initial cellular homogeneity, primary chondrocytes at passage 2 were incubated in 5 mM CellTracker™ green CMFDA in HEPES-supplemented DMEM at 37 °C, 5% CO_2 for 45 min. The cell suspension were then centrifuged at 2000 rpm for 5 min, resuspended in HEPES-supplemented DMEM and incubated at the same condition for an additional 30 min. Next, the cell suspension was centrifuged and resuspended in HEPES-supplemented DMEM at a density of 2.5×10^6 cells/mL. An equal volume of cell suspension was mixed with an equal volume of 1 wt% peptide solution in pH 7.4 buffer (25 mM HEPES) and immediately transferred to 8-well borosilicate plate to allow gel formation. Hydrogels were incubated at 37 °C, 5% CO_2 for 5 h prior to imaging. Images were taken by a Laser Scanning Microscope 710 equipped with a C-Apochromat 10×/0.45 W objective lens (Zeiss, Germany).

For the long term *in vitro* encapsulation study, a 2wt% peptide stock solution was prepared by dissolving lyophilized peptide in pH 7.4 buffer (25 mM HEPES, 340 mM sucrose) at room temperature. 250 μL of the 2 wt% peptide solution was mixed with 750 μL of the cell suspension containing 40×10^6 cell/mL freshly isolated primary chondrocytes in HEPES-supplemented DMEM. The resulting peptide/cell solution containing 0.5 wt% peptide with 30×10^6 cells/mL of chondrocytes was then drawn into a 1-mL syringe equipped with a 21 gauge needle. The loaded syringe was incubated at 37 °C, 5% CO_2 for 10 min to allow hydrogel formation directly within the syringe. Cell-loaded hydrogel was subsequently shear-thin-delivered to 6-mm cell culture inserts (Greiner bio-one, NC) (80–100 μL/insert) placed in a 24-well plate and further incubated at 37 °C, 5% CO_2 for 10 min to allow hydrogel curing. 400 μL of chondrogenic media was added to the top of the hydrogel/cell

constructs and 1 mL of media was placed in the surrounding well. For shape-specific deliveries, cell-loaded hydrogels were drawn onto a 60-mm ultra-low-attachment dish in the shape of the acronym "NCI". Hydrogels were incubated at 37 °C, 5% CO_2 for 10 min to allow hydrogel curing and 6 mL of chondrogenic media was then added to cover the drawn constructs. All constructs were cultured under dynamic condition on an orbital shaker with low agitation. Media was replenished 3 times per week. After 10 days, constructs were transferred to 6-well ultra-low-attachment plates and cultured in the same manner for the remainder of the study.

2.6. Qualitative cell viability

Chondrocyte viability was qualitatively evaluated using a Live/Dead viability/ cytotoxicity kit at 24 h after syringe delivery. A stock solution containing 1 μM calcein AM and 2 μM ethidium homodimer in HEPES-supplemented DMEM was prepared according to package instructions. Gel/cell constructs were first washed in HEPES-supplemented DMEM and then incubated with the dye solution for 15 min at 37 °C, 5% CO_2. Live/dead images were taken by a Laser Scanning Microscope 510 NLO equipped with a Plan-Neofluar 10×/0.3 objective lens (Zeiss, Germany).

2.7. Sample preparation for qualitative and quantitative biochemical and mechanical analysis

At specified time points, gel/cell constructs were collected and prepared for analysis. Fresh constructs were directly used for compression studies without any manipulation. For RNA extraction, constructs were immediately lyophilized and stored at −80 °C. For all other studies, gel/cell constructs were weighed to determine their wet weight, lyophilized, and then weighed again for dry weight determination.

2.8. Biochemical assays

Protease-digested solutions of the constructs were found to interfere with the Hoechst 33258 fluorometric assay and the DMMB spectrophotometric assay for DNA and glycosaminoglycan content, respectively. To eliminate the interference, a modified procedure adapted from a previously published protocol [22] was employed. Briefly, lyophilized constructs were individually pulverized in liq N_2 followed by homogenization in a cold extraction solution (4 M GuHCl, 50 mM Tris, 1mM EDTA pH 8.5). Homogenized samples were vigorously vortex for 30 min at 4 °C and centrifuged at 15,000 g for 10 min at 4 °C. The process of vortex and centrifugation were repeated again, and the GuHCl extract supernatant was stored at −80 °C for further DNA and GAG content measurements.

2.8.1. DNA content—DNA content was determined using a modified Hoechst 33258 fluorometric assay adapted from a previously published protocol [22, 23]. Briefly, 10 μl of the GuHCl extracts (n = 3–4) were mixed with 2 mL of Hoechst 33258 solution (0.2 μg/ mL Hoechst 33258 in 10 mM Tris 1 mM EDTA 200 mM NaCl pH 7.4). The fluorescence of resulting DNA/dye complex were measured by a QuantaMaster spectroflurometer (Photon Technology International, NJ) using 365-nm excitation and 460-nm emission wavelength. DNA content was determined via a standard curve which was generated using sheared DNA calf thymus dissolved in extraction solution (4 M GuHCl, 50 mM Tris, 1 mM EDTA pH 8.5).

2.8.2. Glycosaminoglycan (GAG) content—GAG content was determined using a modified procedure adapted from a previously published procedure [22, 24]. Briefly, the GuHCl extracts (n = 5–6) were diluted in pH 8.5 buffer (50 mM Tris, 1 mM EDTA) resulting in a solution containing 1.6 M GuHCl. Then, 500 μL of DMMB solution was mixed with 50 μL of the diluted GuHCl extract and immediately monitored at A_{525} using an Agilent 8453

UV–Visible spectrophotometer (Agilent Technologies, CA). As a standard, chondroitin sulfate sodium salt from shark cartilage was processed in the same manner as the samples and used to construct a standard curve.

2.8.3. Total collagen content—Total collagen content was determined by the colorimetric measurement of hydroxyproline as previously described [25]. Briefly, lyophilized constructs (n = 4–5) were individually acid-hydrolyzed (2 N HCl at 121 °C) for 15 min and then oxidized by a chloramine-T solution. The resulting solution was reacted with a *p*-dimethylaminobenzaldehyde/ perchloric acid solution. The absorbance of the resulting solutionwas measured at 550 nm (A_{550}) using an Agilent 8453 UV–Visible spectrophotometer (Agilent Technologies, CA). To determine the hydroxyproline content, the absorbance was correlated to a standard curve using Tran-4-hydroxy-L-proline as a standard. Total collagen content was calculated from hydroxyproline content assuming the weight fraction of hydroxyproline in collagen is approximately 13% [26].

2.9. GAG distribution and collagen immunohistochemistry

Gel/cell constructs (n = 3) at 8-week culture were washed 3 times in PBS and fixed in 10% neutral buffer formalin (NBF). Samples were sent to the Pathology and Histotechnology Laboratory, Laboratory Animal Sciences Program, NCI-Frederick (Frederick, MD) for paraffin embedding and sectioning. 5 μm-thick sections were paraffinized in xylene followed by rehydration in 100%, 95% and 70% ethanol respectively. For GAG staining, cell nuclei were stained with Weigert's iron hematoxylin for 4 min, briefly rinsed in fresh acid ethanol (1% conc. HCl in 70% ethanol) followed by tap water. Then, sections were stained with 2% safranin-O solution for 5 min for GAG deposition and briefly rinsed with tap water. For collagen immunohistochemistry staining, slides were incubated in pH 6.0 buffer (10 mM Citrate 0.05% Tween 20) at 92–95 °C for 20 min and allowed to cool down for 30 min. Endogenous hydrogen peroxidase was quenched by 3% hydrogen peroxide in methanol for 10 min. Then the sections were digested in 5 μg/mL proteinase K at 37 °C for 10 min. After blocking with 1% BSA for 30 min, the sections were incubated with either rabbit anti-bovine collagen type I (ab34710, abcam, MA, 1:800) or rabbit anti-bovine collagen type II (ab78482, abcam, MA, 1:100) for 30 min at room temperature. Then, SuperPicture™ HRP staining kit using diaminobenzidine as substrate (Invitrogen, MD) was applied to the sections according to the manufacturer's instruction. The nuclei were stained with Mayer's hematoxylin for 5 min and briefly rinse in ammonia water (0.25% ammonia). The sections stained with safranin-O or immunohistochemistry-stained with collagen antibody were further dehydrated in 70%, 95% and 100% ethanol and cleared with xylene. Sections were mounted with Permount mounting medium and imaged on an Axiovert 40 microscope (Zeiss, Germany).

2.10. Comparative gene expression

At 2, 4, 6, and 8 weeks, lyophilized samples (n = 3) were pooled and pulverized in liq N_2 using a pellet pestle in the presence of TRIZol solution. Total RNA was extracted according to the TRIZol manufacture's protocol. This was followed by DNase treatment using a DNA-free kit (Ambion Inc., TX) according to the package instruction to remove DNA contamination. Total RNA was reverse transcribed to cDNA using an Omniscript RT kit (Qiagen, CA) protocol. A 20 μL reverse transcription reaction consists of 2 μg total RNA, 10 μM random hexamer, 10 unit RNase inhibitor and a recommended concentration of Omniscript reagents. The resultant DNA templates (5 ng) were amplified in a 25 μL real time PCR reaction. Real time PCR reactions were performed using Power SYBR Green PCR Mastermix on a Master Cycle ep *realplex* system (Eppendorf North America, NY). Primer sequences for aggrecan, COL2A1 and COL1A2 are as described in Fitzgerald *et al* [27]. The cycler condition used comprised of incubation for 10 min at 95 °C, followed by 40

cycles of 15 s at 95 °C and 1 min at 60 °C. Dissociation curve analysis was performed at the end of the amplification and PCR products were verified by agarose gel electrophoresis to ensure no non-specific amplification. Comparative gene expression of aggrecan, type I collagen and type II collagen were calculated using a $2^{-\Delta\Delta Ct}$ method [28] with 18s ribosomal RNA as the housekeeping gene and normalized to mRNA extracted from cells encapsulated in MAX8 at 2 weeks. Freshly isolated chondrocytes (P0) and chondrocytes at passage 15 (P15) were also used as controls.

2.11. Mechanical properties

Gel/cell constructs ($n = 4$) at 4 and 8 weeks were collected and the diameter was measured by a digital caliper. Unconfined compression analysis was performed at room temperature using an ARES-G2 rheometer (TA Instruments, DE) equipped with an immersion chamber. Each construct was placed between stainless steel parallel plates and immersed in PBS. The samples were subjected to a ramp of 2% strain compression in 20 s (0.1% strain/s), followed by a 20 min relaxation. This was repeated for a total of 6 cycles. The equilibrium modulus was calculated as the slope of relaxed equilibrium stress as a function of its respective strain.

2.12. Data analysis

Average data ± standard deviations are shown for all data sets. Statistical analysis between two experimental groups (i.e. different peptides or same peptide at different time points) was assessed by a two-tailed unpaired *t*-test using the Graphpad Prism 5.0 software package.

3. Results and discussion

3.1. Peptide design

This study necessitates the preparation of two peptide-based networks of differing electrostatic character, yet similar in other attributes that might influence cell behavior. The design of the peptides used in this study was guided by several criteria. First, each peptide must self-assemble at a similar rate to yield well-defined fibrillar networks of similar morphology. This ensures that cells experience similar local network conditions during encapsulation. Secondly and most difficult, both peptides must form hydrogels having similar storage moduli. This ensures that cells experience similar material stiffness when encapsulated in each gel. Third, each gel must display similar shear-thin/recovery behavior so that cells experience similar microenvironments during delivery. Adhering to these design criteria ensures that any differences in cell behavior between the two networks are largely due to electrostatics and not other material attributes.

The parent peptide used in this study is MAX8, Table 1. This peptide forms moderately stiff gels at low weight percent that display shear-thin/recovery behavior. In addition, we have previously shown that gels composed of MAX8 are cytocompatible toward multiple cell lines [10, 11]. MAX8 is a twenty-residue peptide designed to adopt an ensemble of random coil conformations when dissolved in low ionic strength aqueous buffer at pH 7.4. Under these solution conditions, the lysine residue side chains are protonated and the resulting intra-residue charge repulsion inhibits peptide folding. Solutions of unfolded peptide have the viscosity of water. However, the addition of cell culture media to a solution of unfolded peptide triggers intramolecular peptide folding. The inherent salt content of the media screens the lysine-borne charge and allows the peptide to fold into an amphiphilic β-hairpin conformation, see Fig. S1 in Supporting Information. In the folded state, MAX8 contains two β-strands that form a network of intramolecular hydrogen bonds. The two strands are covalently connected by a four-residue type II′ β-turn (-V^{D}PPT-) that ensures chain reversal when folding is initiated. Each strand region contains an alternating sequence of hydrophobic and hydrophilic residues giving the hairpin its amphiphilic character. MAX 8

also contains a glutamic acid on its hydrophilic face, at position 15, that is capable of forming a salt bridge with a neighboring lysine residue across the hairpin at position 6, further stabilizing the folded conformation.

The folded hairpin is highly amenable to self-assembly. It assembles laterally via intermolecular hydrogen bond formation along the long axis of a growing fibril. In addition, the intra-molecular salt bridge formed in the folded monomer evolves into a network of intermolecular salt bridges during self-assembly. The network runs along the long axis of a given fibril on both its water exposed faces. MAX8 also assembles facially, where the hydrophobic faces of two distinct hairpins associate to form a bilayer where the large hydrophobic surface area of each hairpin is shielded from water. Facial assembly is largely governed by the hydrophobic affect, which is temperature-dependent, and favored at higher temperatures. Thus, the hydrophobic association of hairpins during bilayer formation provides the thermodynamic driving force for self-assembly. Whereas, intermolecular hydrogen bond and salt bridge formation dictates strand registry and provides structural specificity to the self-assembled state, ensuring the formation of a homogenous population of well-defined fibrils.

Peptide folding is largely governed by the alleviation of side chain charge repulsion, which allows the side chains of the hydrophilic residues to approach each other during folding to form the hydrophilic face of the hairpin. Changes in peptide sequence on the hydrophilic face of the hairpin that lowers its overall charge state will promote peptide folding. Conversely, changes that increase the charge state make folding more difficult because more positive charge must be screened when folding is triggered. To a large extent, self-assembly is thermodynamically driven by the association of hydrophobic side chains. Sequence changes on the hydrophobic face of the hairpin that increase its hydrophobic content, promote its self-assembly. Conversely, decreasing the hydrophobic content on this face decreases the driving force for self-association. However, it must be kept in mind that peptide folding and self-assembly are, most likely, linked equilibria. As a result, these effects are not mutually exclusive and making changes to the peptide's sequence that are designed to largely influence folding will certainly also effect self-assembly to some degree and vice-versa. Thus, designing two peptides that display different overall charge states at a common pH without significantly altering their rates of gelation and the mechanical properties of their resulting gels, presents a unique design challenge.

Using MAX8 as the parent peptide, we set out to design a new sequence that would ultimately form a less electropositive hydrogel network. MAX8 has a net positive charge of +7 when dissolved in pH 7.4 buffer, due to its seven lysine residues, N-terminal amine group and its lone glutamic acid residue at position 15, Table 1. We envisioned that the design of a new peptide having an overall charge state of +5 at neutral pH, would assembled into a gel having a significantly lower electropositive potential. Although a change of two charge units per monomeric peptide may seem modest, a hydrogel network formed by a large copy number of self-assembled peptides (e.g. 0.5 wt%, ~1.7 m_M) magnifies this difference. In addition, the design of such a peptide should be tractable with an iterative-based design starting from a known sequence.

Conceptually, the most straightforward manner in which to reduce the overall charge of MAX8 by two charge units is to simply replace one of its positively charged lysine residues with a negatively charged residue. Thus, the lysine at position 4 was replaced with a glutamic acid to produce HE1 (Hairpin Glutamate (E)-1), a peptide having an overall charge of +5 at neutral pH, Table 1. A glutamic acid incorporated at this position would have the potential to form an intramolecular salt bridge with the lysine across the hairpin at position 17. Alternatively, incorporating the glutamic acid at position 17 could, in principle,

accomplish the same effect by forming a salt bridge with the existing lysine at position 4. However, incorporating the Glu at position 17 might induce a repulsive charge interaction with the existing glutamate at position 15 and destabilize the folded state. At any rate, HE1 was designed to form two salt bridges in the folded state and a dual network of salt bridges in the self-assembled state. Folding and self-assembly should occur more quickly for HE1 relative to MAX8 since less positive charge needs to be screened to enable folding and an addition salt bridge network will be formed during assembly. Unfortunately, when cell culture media was added to buffered solutions (pH 7.4) of HE1 to initiate folding and self-assembly, the peptide rapidly precipitates from solution, instead of forming a well-behaved hydrogel. Thus, incorporation of a glutamic acid residue at position 4 in the context of MAX8 is detrimental to gelation. This change most likely enables alternant self-assembly pathways to occur that lead to higher order structures and resultant precipitation.

As a result, the lysine residue was restored to position 4 and other design strategies were pursued. To avoid installing additional negatively charged residues on the hairpin's hydrophilic face, such as in HE1, we explored replacing several lysine residues with neutral amino acids. In the peptide HIT1 (Hairpin IsoleucineThreonine-1), the two terminal lysine residues of MAX8 at positions 2 and 19 were replaced with two isoleucine residues. Such a change would reduce the charge state to +5. Isoleucine was chosen based on its known propensity to adopt dihedral angles consistent with β-structure [29]. Positions 2 and 19 were chosen to house these residues since they are non-hydrogen bonded positions located directly across from each other near the terminus of the hairpin. Naturally occurring β-sheet proteins will often position hydrophobic residues directly across the sheet from each other where they can form a cross-strand, pair-wise interaction [30]. In the idealized case, each residue extends its side chain across the β-sheet to form a nested hydrophobic contact, much like two hands greeting each other in a friendly shake. In the context of the hairpin, in addition to lowering the overall charge state of the peptide, the formation of such an interaction could possibly stabilize the folded state by stapling the N- and C-terminal regions of each strand together. Lastly, since these changes would likely result in a peptide that would fold and assemble much more quickly than MAX8, one additional change to the sequence was made. Namely, the valine at position 3 of the hairpin was replaced with the more polar, but isostructural residue, threonine. This change decreases the hydrophobic content on the hydrophobic face of the hairpin and should decrease the rate of assembly. HIT1 was synthesized using standard Fmoc-based solid-phase synthesis. Although the synthesis of crude HIT1 is tractable, its purification by reverse-phase-HPLC is extremely difficult due its high hydrophobic content. Its poor behavior on the purification column served as a prelude to its behavior in solution. The small amount of HIT1 that could ultimately be purified by herculean efforts quickly precipitated from solution when peptide folding and assembly was triggered by the addition of cell culture media. This poor behavior is presumably due to the peptide's high hydrophobic content. Gratifyingly, one small change was sufficient to circumvent this problem. Namely, an additional valine on the hydrophobic face at position 7 was replaced with threonine to further lower the hydrophobic content of the peptide. The resulting peptide, HIT2 could be synthesized and purified in large amounts, was not prone to precipitation and could form self-supporting gels.

Fig. 1A shows time-sweep oscillatory rheology data that monitors the onset of gelation for 0.5 wt% HIT2 compared to MAX8. In this experiment, DMEM cell culture media is added to buffered solutions (25m_M HEPES, pH 7.4) of unfolded peptide. Gel formation is accompanied by an increase in the measured storage modulus (G'). When triggered, HIT2 forms a weak gel over the time span of several minutes that further stiffens with time yielding a G' of 245 ± 27 Pa after 1 h. In comparison, under identical conditions, MAX8 is capable of rapid gelation forming a network characterized by a G' of 763 ± 18 Pa after 1 h. Thus, the rate of gelation for HIT2 is notably slower and the mechanical rigidity of its

resulting gel is significantly different with respect to MAX8. As a consequence, HIT2 failed to meet the design criteria discussed earlier.

We surmised that HIT2's slow rate of gelation was due to the incorporation of the additional threonine at position 7, which ultimately decreased the hydrophobic content on the hydrophobic face of the hairpin. Its logical to expect that a future design might simply include replacing this threonine with a more hydrophobic residue. However, we feared that not only would such a change result in a faster assembler, which is desired, but could also yield a peptide with the same purification and precipitation problems as HIT1. Thus, the threonine at position 7 was left intact and attention was returned to the nested hydrophobic interaction between the isoleucine residues at positions 2 and 19. Molecular modeling suggested that if two leucine residues were incorporated at these positions, instead of the two isoleucines, better side chain packing could occur between the nested leucines and the methylene portions of the two adjacent lysines on the hydrophilic face, See Supporting Information. Such an enhancement in side chain packing might be able to stabilize the transition state leading to the folded conformation, ultimately increasing the rate of folding. And because folding and self-assembly are linked equilibria, the rate of assembly leading to gelation might also increase.

Thus, the sequence of HLT2 features two leucines and a net positive charge of +5 at neutral pH, Table 1. HLT2 is well-behaved during purification and solutions of unfolded peptide undergo gelation at a rate comparable to MAX8 when triggered with cell culture media, Fig. 1A. In addition, the storage modulus of the HLT2 gel (566 ± 76 Pa) is similar to that of the MAX8 gel (763 ± 18 Pa) after 1 h. Further rheological studies were performed to investigate the shear thinning and recovery properties of the HLT2 gel as compared to the MAX8 gel. Fig. 1B shows an oscillatory rheology experiment, where hydrogelation was triggered by the addition of DMEM cell culture media and each gel allowed to form over a 10-min period. Next, 1000% strain was applied for 30 s to each gel in order to thin the materials. During the thinning process, both peptide gels display a rapid decrease in G', indicating that both are converted from moderately rigid gels to low viscosity gels capable of flow. After the 30-s thinning period, the strain was reduced to 0.2%, at which time both gels recover, with a rapid increase in their respective storage moduli to values nearly identical to those realized before thinning.

The comparative rheological data indicate that HLT2 and MAX8, although different in sequence and charge state, form gels of similar mechanical rigidity at similar rates, and each gel is capable of recovering after shear thinning. Thus, each gel should be capable of encapsulating and shear-thin delivering cells in a similar manner. This assertion was qualitatively tested by directly encapsulating and syringe-delivering primary bovine chondrocytes to assess cellular distribution at the inject site. In this *ex vivo* experiment, chondrocytes were labeled with CellTracker™ green DMFDA and directly encapsulated at a cell density of 1.25×10^6 cells/mL in both MAX8 and HLT2 hydrogels. Cells were encapsulated by simply adding a suspension of cells in DMEM to a buffered solution of unfolded peptide, quickly drawing the gelling solution into a syringe and allowing the resulting gel-cell construct to rigidify in the syringe at 37 °C. Solid gel-cell constructs were then syringe-delivered to an imaging well. The lower cell seeding density was chosen to minimize fluorescence interference and allow relatively thick (1 mm) samples to be imaged. Fig. 1C shows Z-stacked confocal micrographs viewed perpendicular to the *Z*-axis of the gelcell constructs 5 h after syringe delivery. Primary chondrocytes are homogeneously encapsulated within both the MAX8 and HLT2 hydrogels with similar cellular densities.

Lastly, transmission electron microscopy (TEM) was used to probe the local structure of the fibrils formed by both MAX8 and HLT2. Fig. S3 shows that each peptide self-assembles to

form well-defined fibrils that are approximately 3 nm in diameter, which corresponds to the width of a folded hairpin in the self-assembled state. Thus, both MAX8 and HLT2 fold and self-assemble, forming fibrils of similar morphology.

Taken together, the rheological, TEM, and cellular distribution data suggest that HLT2 and MAX8 should provide similar microenvironments during the encapsulation and delivery of cells with the important difference of network electrostatics. With these two peptide gels in hand, the influence of network electropositive character on primary chondrocyte behavior could be investigated.

3.2. Comparative in vitro studies

Comparative *in vitro* studies were performed to investigate the response of primary bovine chondrocytes to the MAX8 and HLT2 hydrogels in the absence of any exogenous growth factors, cytokines and extracellular matrix molecules. In the following studies, freshly isolated cells were encapsulated in either 0.5 wt% MAX8 or HLT2 hydrogels. The encapsulated chondrocytes were syringe-delivered to tissue culture wells and cultured *in vitro*. The influence of network electrostatics on cell viability after encapsulation and delivery, extracellular matrix deposition, gene expression, and the bulk mechanical properties of the gel-cell constructs as a function of culture time was assessed.

3.2.1. Cell viability—The viability of chondrocytes encapsulated in MAX8 and HLT2 hydrogels was qualitatively assessed 24 h after syringe delivery using a Live-Dead assay, where live cells are stained with calcein AM (green) and dead cells are stained with ethidium homodimer (red). Fig. 2A shows a confocal Z-stacked micrograph of cells viewed along the *z*-axis. The depth of the image plane is approximately 100 microns. The image shows that the majority of cells delivered using the MAX8 hydrogel remain viable. However, there is a significant population of non-viable cells at 24 h. However, Fig. 2B suggests that the less electropositive network of HTL2 results in an increase in the number of viable cells. Cell viability was then assessed quantitatively by measuring the DNA content of each gel-cell construct as a function of time, Fig. 2C. For both gels, cells proliferated during the first 2 weeks post delivery as indicated by an increase in the DNA content from 20 μg/construct (assuming 7.7 pg/cells [31]) at day 0–40.03 ± 5.24 μg/construct and 48.12 ± 4.04 μg/construct at day 14 for MAX8 and HLT2 gels, respectively. DNA content increased modestly until leveling out after 6 weeks for the HLT2 gel, whereas DNA content in the MAX8 gel changed little over the time course of the study. Interestingly, HLT2 constructs contained more DNA content as compared to MAX8 constructs at every time point. After 8 weeks of culturing, the MAX8 constructs contained significantly less DNA as compared to the HLT2 constructs. This difference is consistent with the qualitative live-dead assay and suggests that the less electropositive network provided by HLT2 is more conducive to cell viability.

3.2.2. Extracellular matrix deposition—Primary chondrocytes are known to dedifferentiate once they are removed from their native environment and cultured *in vitro* [32, 33]. A common characteristic of dedifferentiated cells is a change in morphology from a spherical shape to a spread-out, fibroblastic-like shape. This change in morphology is accompanied by a down-regulation of cartilage-specific genes such as aggrecan, a proteoglycan core protein, and type II collagen, as well as an up-regulation of type I collagen. As a result, tissue-engineered cartilage cultured *in vitro* is typically inferior in mechanical properties as compared to that of native articular cartilage with a substantially lower glycosaminoglycan (GAG) and type II collagen content. The ability of cells to elaborate GAG and collagen after being delivered from MAX8 and HLT2 gels was quantitatively measured as a function of time, Fig. 3. In panel A, it is evident that GAG

content is significantly greater in the HLT2 construct at every time point. After 8 weeks, HLT2 constructs contain 103.3 13.2 μg of GAG per mg dry weight of construct. In comparison, the MAX8 constructs yield 81.2 7.3 μg GAG/mg dry weight. Panel B shows a similar trend for total collagen, with accumulation being greater in the HLT2 construct at every time point. At 8 weeks, 21.6 ± 1.9 μg collagen/mg dry weight was observed in HLT2 while 16.5 ± 2.0 μg collagen/mg dry weight was observed in MAX8 constructs.

Histological assessment of gel-cell constructs was performed at 8 weeks to provide additional information on the gross content of GAG, type I and II collagen as well as the spatial distribution of these cartilage markers within the construct. In agreement with the quantitative measurements, safranin-O staining shows that a modest level of GAG had been non-uniformly deposited within the MAX8 construct, Fig. 4A. However, there is greater GAG accumulation with even distribution in the HLT2 constructs, Fig. 4B.

Immunohistochemical staining of type I and type II collagen was also performed. The accumulated collagen within both MAX8 and HLT2 constructs was found to be a combination of type I and type II collagen. Type II collagen, a hyaline cartilage-specific collagen, was distributed throughout the HLT2 constructs (Fig. 4D). In contrast, minimal deposition of type II collagen was observed in MAX8 constructs (Fig. 4C). Type I collagen, a typical marker of dedifferentiated chondrocytes, was observed in both MAX8 and HLT2 constructs but predominantly accumulated on the peripheral of the constructs (Fig. 4E and F). The data also show that cells delivered and cultured in the HLT2 gel deposit significantly more total collagen than those in the MAX8 gel (compare cumulatively panels D and F to panels C and E). This is in agreement with the quantitative data presented in Fig. 3B. Also evident is that the collagen deposited in the MAX 8 construct is distributed unevenly and is predominantly type I (compare panels C and E). Collagen deposited in the HLT2 construct is more evenly distributed and is a mixture of both type I and II. The data in Figs. 3 and 4taken together, suggest that primary chondrocytes are capable of producing both GAG and collagen in both constructs, but do so more in the less electropositive HLT2 gel. Based on the immunohistochemical data, cells in both gels produce significant amounts of type I collagen, presumable due to dedifferentiation of the primary chondrocytes to the fibroblast-like phenotype. This assertion was studied further by examining the morphology of cells in both gel constructs.

3.2.3. Cell morphology—The dedifferentiation of chondrocytes to a fibroblast-like phenotype is accompanied by a transition in cellular morphology from round to spread-out. The insets in Fig. 4 show the morphology of cells within different regions of each of the constructs. It's obvious that cells have undergone dedifferentiation in both the MAX8 and HLT2 gels, examples are indicated by the red arrows in the figure. Qualitative assessment of the images suggests that the extent of dedifferentiation is greater in the MAX8 hydrogel. The insets in panels A and B are magnifications of regions near the center (as opposed to their edges) of the circularly shaped constructs. For the most part, cells contained in this region within the HLT2 gel seem to retain their chondrocytic phenotype, as indicated by the green arrows, with a small percentage adopting the fibroblastic phenotype. In contrast, the center region of the MAX8 construct contains a large number of dedifferentiated cells. Magnifications of the edges of the constructs are shown in Panels C–F. The outer edges of both gels contain large populations of dedifferentiated cells, which is consistent with the immunohistochemical data showing that this region contains a high concentration of type I, but not type II collagen, Panels C–F. It should be noted that the relatively high levels of dedifferentiation at the outer edges of both gels is expected and is commonly observed in other types of hydrogels reported in the literature [34–36], especially those used under static culturing conditions. In our study, dynamic conditions were not employed, and the experimental methodology was kept simple to focus the study on elucidating the influence

of network electrostatics on cell behavior. The purpose of our study was not to optimize culture conditions for the *in vitro* production of articular cartilage. At any rate, the analysis of the ECM deposited in each gel correlates well with the observed changes in cellular morphology, and suggests that network electrostatics influences cell behavior for this class of peptide-based gels.

3.2.4. Relative gene expression—An analysis of the relative expression of genes important in cartilage elaboration was performed to compliment the quantitative analysis of cartilage-specific ECM components and the histology. Gene expression levels were measure as a function of culture time for cells encapsulated and delivered via the MAX8 and HLT2 gels. Cells encapsulated in both hydrogels show a decrease in aggrecan and type II collagen expression levels at 2 and 4 weeks as compared to levels measured in freshly isolated cells (Passage 0), Fig. 5A and B. Expression levels increased slightly after 6 weeks for cells in both gels with levels being slightly higher for those in the HLT2 gel. Fig. 5C shows that gene expression levels of type I collagen were up-regulated in both MAX8 and HLT2 hydrogels as compared to fully dedifferentiated chondrocytes that were culture to passage 15 (P15), indicating that a large number of cells dedifferentiated as suggested by the immunohistochemical data and the assessment of cell morphology discussed earlier. Importantly, differences between the relative expression levels of all the genes studied here are realized when comparing the MAX8 and HLT2 networks, again, supporting that network electrostatics is influencing cell behavior.

3.2.5. Mechanical differences of MAX8 and HLT2 constructs—The cell-based data presented thus far indicates that primary chondrocytes encapsulated and delivered using the less electropositive HLT2 gel are better able to preserve their phenotype. Cells are able to produce greater amounts of more evenly distributed GAG as well as total collagen, with the relative amount of type II versus type I being slightly higher in the HLT2 gel. As such, the HLT2-cell construct should demonstrate measurably better mechanical properties than the MAX8 construct. After cells are encapsulated and delivered, the evolution of the bulk mechanical properties can be qualitatively and quantitatively assessed. Qualitatively, ECM elaboration and change in the mechanical properties can be visualized during the culturing of the gel-cell constructs. When encapsulated chondrocytes are initially syringe-delivered onto the membranes of cell culture inserts, they are mechanically soft and conform to the shape of the insert. After 5–6 days, the HLT2 constructs become rigid and begin to float out from the insert. These self-supportive, macroscopic constructs can be cultured in suspension independent of the support of the membrane. In contrast, MAX8 constructs take over 10 days to display the same behavior. Although extremely qualitative, this observation provides insight into the rate of ECM deposition for both gel networks. Fig. 6A shows examples of the circular constructs that result from initially injecting the gel containing cells into confined circular inserts. After the constructs lift from their respective insert they grow in size but retain their shape. After 8 weeks, constructs derived from HLT2 gels are reproducibly larger then those derived from MAX8 gels ($p < 0.001$). The average diameter of MAX8 constructs were 5.80 ± 0.12 mm while HLT2 construct were 6.61 ± 0.19 mm ($n = 4$). Fig. 6B shows the result of syringe injecting encapsulated cells into non-confined injection sites. Here, gel-cell constructs derived from both HLT2 and MAX8 are syringe-delivered to a low-attachment tissue culture surface and initially drawn in the shape of the letters ‘NCI’ (drawn from bottom to top to ensure continuity of flow). The rate of ECM deposition is nicely evident in this experiment. Both gel-cell constructs retain their shape after initial delivery. However, chondrocytes encapsulated in the HLT2 hydrogel required less time to establish a self-supportive construct as compared to the MAX8 hydrogel. Interestingly, after 8 weeks, the HLT2 construct remained intact and maintained its shape

and integrity as drawn with a slight increase in its volume. In comparison, the MAX8 construct failed to maintain its initial shape, collapsing onto itself during culture.

To quantitatively assess the mechanical properties of the circular gel-cell constructs, their equilibrium moduli was measured via unconfined compression at 4 and 8 weeks in PBS at room temperature. Fig. 7 shows data for four individual gel-cell constructs for both MAX8 and HLT2. At each time point, the HLT2 constructs exhibited greater equilibrium moduli than those measured for the MAX8 constructs. The MAX8 constructs showed very little increase in their equilibrium moduli over time with an average of 2.25 ± 0.57 kPa at 4 weeks and 2.55 ± 1.17 kPa at 8 weeks. On the other hand, the HLT2 constructs showed an increase in their equilibrium moduli from 3.90 ± 0.74 kPa at 4 weeks to 5.55 ± 0.39 kPa at 8 weeks ($p < 0.01$). The higher moduli afforded by the HLT2 constructs may, in part, be due to the better response of encapsulated chondrocytes leading to greater GAG and total collagen deposition as shown earlier. This data clearly demonstrates that cells encapsulated, delivered and cultured in MAX8 and HLT2 gels yield mechanically different tissue constructs, suggesting that changes in the electropositive environment of the network influence chondrocyte behavior.

The influence of network electrostatics on cell behavior can result from a number of factors. For example, deleterious ionic interactions between the charged material network and membrane-bound cell surface proteins and oligosaccharides could impair or augment cell behavior. Also, the physical adsorption of essential soluble factors, such as growth factors and cytokines, to the gel network could limit the intended effect of these molecules, thereby augmenting cell behavior. It should also be noted that although the HLT2 gel performed better than the MAX8 gel in the context of delivering and culturing chondrocytes, the intent of this study was not to design the optimal gel for this application, but rather to investigate how network electrostatics might influence cell behavior. In fact, the static culturing methods employed here are extremely basic and thus, the data presented provides little indication of how well these gel-cell constructs will perform in an *in vivo* context. Indeed, based on the *in vitro* data presented here, it is likely that other peptide sequences may provide gels that perform much better.

The work presented here also brings up another interesting proposition concerning the design of materials for use in delivering different types of cells. Given the complexity and differences in each cell type's microenvironment, it is probable that no one material will fit the bill for all or even most cells. More likely, a plethora of different materials will have to be designed to accommodate each cell's proper delivery; in essence, personalized health care for cells. In fact, we have shown previously that the MAX8 gel is cytocompatible towards murine mesenchymal stem cells [10] and MG63 cells [11], which is in contrast to the response of the bovine primary chondrocytes used in this study.

4. Conclusions

Herein, iterative peptide design was used to generate two peptide-based gels that were used to study the effect of network electrostatics on chondrocyte behavior. MAX8 and HLT2 peptides have formal charge states of +7 and +5 per monomer at neutral pH. These peptides undergo environmentally triggered folding and self-assembly to afford hydrogel networks having similar mechanical properties yet different electropositive character. Each gel can be used to directly encapsulate and syringe-deliver primary chondrocytes. Assessment of cell viability and morphology, extracellular matrix deposition and the mechanical properties of cultured gel-cell constructs show that network electrostatics influences cell behavior for these peptide-based materials. The less electropositive HLT2 gel is better able to support chondrocyte encapsulation, delivery, and maintenance of phenotype. As a result, gel-cell

constructs prepared with HLT2, cultured under static *in vitro* conditions contained more GAG and type II collagen resulting in mechanically superior constructs. Chondrocytes delivered in the more electropositive MAX8 gel experienced a greater degree of cell death during encapsulation and delivery and the remaining viable cells were less prone to maintain their phenotype. As a result, MAX8 gel-cell constructs had fewer cells, of which a limited number were capable of laying down cartilage-specific ECM.

Supplementary Material

Refer to Web version on PubMed Central for supplementary material.

Acknowledgments

We thank Dr. Weidong Yang and Dr. Sonia D'Souza for technical assistance. We also thank Dr. Mary C. Farach-Carson for fruitful discussion. This work is partially supported by a graduate fellowship awarded to Chomdao Sinthuvanich through the Strategic Scholarship for Frontier Research Network (SFR) from the Office of the Higher Education Commission, Ministry of Education, Thailand. Research funding was provided by the Intramural Research Program of the National Cancer Institute, National Institutes of Health.

References

1. Vaquero J, Forriol F. Knee chondral injuries: clinical treatment strategies and experimental models. Injury. 2012; 43(6):694–705. [PubMed: 21733516]
2. Farr J, Cole B, Dhawan A, Kercher J, Sherman S. Clinical cartilage restoration: evolution and overview. Clin Orthop Relat Res. 2011; 469(10):2696–2705. [PubMed: 21240578]
3. Brittberg M, Lindahl A, Nilsson A, Ohlsson C, Isaksson O, Peterson L. Treatment of deep cartilage defects in the knee with autologous chondrocyte transplantation. N Engl J Med. 1994; 331(14):889–895. [PubMed: 8078550]
4. Riegger-Krugh CL, Mccarty EC, Robinson MS, Wegzyn DA. Autologous chondrocyte implantation: current surgery and rehabilitation. Med Sci Sports Exerc. 2008; 40(2):206–214. [PubMed: 18202583]
5. Iwasa J, Engebretsen L, Shima Y, Ochi M. Clinical application of scaffolds for cartilage tissue engineering. Knee Surg Sports Traumatol Arthrosc. 2009; 17(6):561–577. [PubMed: 19020862]
6. Amini AA, Nair LS. Injectable hydrogels for bone and cartilage repair. Biomed Mater. 2012; 7(2)
7. Zheng Shu X, Liu Y, Palumbo FS, Luo Y, Prestwich GD. In situ crosslinkable hyaluronan hydrogels for tissue engineering. Biomaterials. 2004; 25(7–8):1339–1348. [PubMed: 14643608]
8. Aguado BA, Mulyasasmita W, Su J, Lampe KJ, Heilshorn SC. Improving viability of stem cells during syringe needle flow through the design of hydrogel cell carriers. Tissue Eng Part A. 2011; 18(7–8):806–815. [PubMed: 22011213]
9. Engler AJ, Sen S, Sweeney HL, Discher DE. Matrix elasticity directs stem cell lineage specification. Cell. 2006; 126(4):677–689. [PubMed: 16923388]
10. Haines-Butterick L, Rajagopal K, Branco M, Salick D, Rughani R, Pilarz M, et al. Controlling hydrogelation kinetics by peptide design for three-dimensional encapsulation and injectable delivery of cells. Proc Natl Acad Sci U S A. 2007; 104(19):7791–7796. [PubMed: 17470802]
11. Yan C, Mackay ME, Czymmek K, Nagarkar RP, Schneider JP, Pochan DJ. Injectable solid peptide hydrogel as a cell carrier: effects of shear flow on hydrogels and cell payload. Langmuir. 2012; 28(14):6076–6087. [PubMed: 22390812]
12. Schneider JP, Pochan DJ, Ozbas B, Rajagopal K, Pakstis L, Kretsinger J. Responsive hydrogels from the intramolecular folding and self-assembly of a designed peptide. J Am Chem Soc. 2002; 124(50):15030–1507. [PubMed: 12475347]
13. Rajagopal K, Lamm MS, Haines-Butterick LA, Pochan DJ, Schneider JP. Tuning the pH responsiveness of β-hairpin peptide folding, self-assembly, and hydrogel material formation. Biomacromolecules. 2009; 10(9):2619–2625. [PubMed: 19663418]

14. Branco MC, Pochan DJ, Wagner NJ, Schneider JP. The effect of protein structure on their controlled release from an injectable peptide hydrogel. Biomaterials. 2010; 31(36):9527–9534. [PubMed: 20952055]
15. Fischer D, Li Y, Ahlemeyer B, Krieglstein J, Kissel T. In vitro cytotoxicity testing of polycations: influence of polymer structure on cell viability and hemolysis. Biomaterials. 2003; 24(7):1121–1131. [PubMed: 12527253]
16. Schneider GB, English A, Abraham M, Zaharias R, Stanford C, Keller J. The effect of hydrogel charge density on cell attachment. Biomaterials. 2004; 25(15):3023–3028. [PubMed: 14967535]
17. Xu Y, Takai M, Ishihara K. Protein adsorption and cell adhesion on cationic, neutral, and anionic 2-methacryloyloxyethyl phosphorylcholine copolymer surfaces. Biomaterials. 2009; 30(28):4930–4938. [PubMed: 19560198]
18. Keselowsky BG, Collard DM, Garcıa AJ. Surface chemistry modulates focal adhesion composition and signaling through changes in integrin binding. Biomaterials. 2004; 25(28):5947–5954. [PubMed: 15183609]
19. Chen YM, Gong JP, Tanaka M, Yasuda K, Yamamoto S, Shimomura M, et al. Tuning of cell proliferation on tough gels by critical charge effect. J Biomed Mater Res A. 2009; 88A(1):74–83. [PubMed: 18260145]
20. Dadsetan M, Pumberger M, Casper ME, Shogren K, Giuliani M, Ruesink T, et al. The effects of fixed electrical charge on chondrocyte behavior. Acta Biomater. 2011; 7(5):2080–2090. [PubMed: 21262395]
21. Guo L, Kawazoe N, Hoshiba T, Tateishi T, Chen G, Zhang X. Osteogenic differentiation of human mesenchymal stem cells on chargeable polymer-modified surfaces. J Biomed Mater Res A. 2008; 87A(4):903–912. [PubMed: 18228270]
22. Hoemann CD, Sun J, Chrzanowski V, Buschmann MD. A multivalent assay to detect glycosaminoglycan, protein, collagen RNA, DNA content in milligram samples of cartilage or hydrogel-based repair cartilage. Anal Biochem. 2002; 300(1):1–10. [PubMed: 11743684]
23. Labarca C, Paigen K. A simple, rapid, and sensitive DNA assay procedure. Anal Biochem. 1980; 102(2):344–352. [PubMed: 6158890]
24. Chandrasekhar S, Esterman MA, Hoffman HA. Microdetermination of proteoglycans and glycosaminoglycans in the presence of guanidine hydrochloride. Anal Biochem. 1987; 161(1):103–108. [PubMed: 3578776]
25. Kesava Reddy G, Enwemeka CS. A simplified method for the analysis of hydroxyproline in biological tissues. Clin Biochem. 1996; 29(3):225–229. [PubMed: 8740508]
26. Ignat'eva N, Danilov N, Averkiev S, Obrezkova M, Lunin V, Sobol' E. Determination of hydroxyproline in tissues and the evaluation of the collagen content of the tissues. J Anal Chem. 2007; 62(1):51–57.
27. Fitzgerald JB, Jin M, Grodzinsky AJ. Shear and compression differentially regulate clusters of functionally related temporal transcription patterns in cartilage tissue. J Biol Chem. 2006; 281(34):24095–24103. [PubMed: 16782710]
28. Livak KJ, Schmittgen TD. Analysis of relative gene expression data using real-time quantitative PCR and the $2^{-\Delta\Delta CT}$ Method. Methods. 2001; 25(4):402–408. [PubMed: 11846609]
29. Minor DL, Kim PS. Measurement of the β-sheet-forming propensities of amino acids. Nature. 1994; 367(6464):660–663. [PubMed: 8107853]
30. Wouters MA, Curmi PMG. An analysis of side chain interactions and pair correlations within antiparallel b-sheets: the differences between backbone hydrogen-bonded and non-hydrogen-bonded residue pairs. Proteins Struct Funct Bioinformat. 1995; 22(2):119–131.
31. Kim Y-J, Sah RLY, Doong J-YH, Grodzinsky AJ. Fluorometric assay of DNA in cartilage explants using Hoechst 33258. Anal Biochem. 1988; 174(1):168–176. [PubMed: 2464289]
32. Lin Z, Fitzgerald JB, Xu J, Willers C, Wood D, Grodzinsky AJ, et al. Gene expression profiles of human chondrocytes during passaged monolayer cultivation. J Orthop Res. 2008; 26(9):1230–1237. [PubMed: 18404652]
33. Schuh E, Hofmann S, Stok K, Notbohm H, Müller R, Rotter N. Chondrocyte redifferentiation in 3D: the effect of adhesion site density and substrate elasticity. J Biomed Mater Res A. 2012; 100A(1):38–47. [PubMed: 21972220]

34. Hoemann CD, Sun J, Légaré A, McKee MD, Buschmann MD. Tissue engineering of cartilage using an injectable and adhesive chitosan-based cell-delivery vehicle. Osteoarthritis Cartilage. 2005; 13(4):318–329. [PubMed: 15780645]

35. Tare RS, Howard D, Pound JC, Roach HI, Oreffo ROC. Tissue engineering strategies for cartilage generation—Micromass and three dimensional cultures using human chondrocytes and a continuous cell line. Biochem Biophys Res Commun. 2005; 333(2):609–621. [PubMed: 15946652]

36. Akmal M, Anand A, Anand B, Wiseman M, Goodship AE, Bentley G. The culture of articular chondrocytes in hydrogel constructs within a bioreactor enhances cell proliferation and matrix synthesis. J Bone Jt Surg Br. 2006; 88-B(4):544–553.

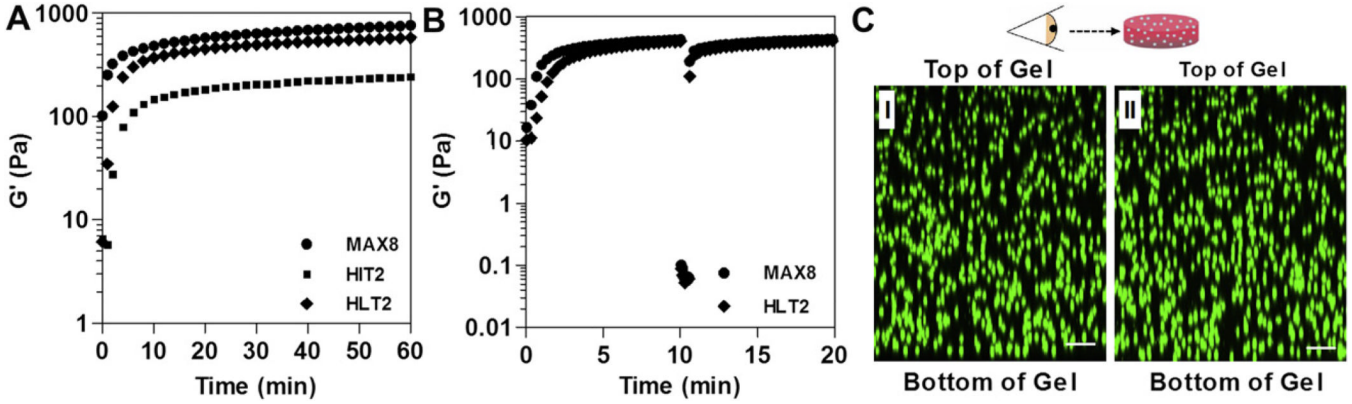

Fig. 1.

Rhelogical properties of 0.5 wt% peptide gels (25 mM HEPES 0.5× DMEM pH 7.4, 37 °C). (A) Dynamic time sweeps (frequency = 6 rad/s, 0.2% strain) of MAX8, HIT2 and HLT2 hydrogels. (B) Shear-thin recovery of MAX8 and HLT2 gels; the first 10 min represents the onset of gelation (0.2% strain, 6 rad/s). After which, gels are shear-thinned at 1000% strain for 30 s and allowed to recover by reducing the strain to 0.2%. (C) Distribution of primary chondrocytes in 0.5 wt% MAX8 (I) or HTL2 (II) hydrogels after syringe delivery. Cells were labeled with CellTracker™ green CMFDA and encapsulated at a density of 1.25×10^6 cells/mL. LSCM images were taken at 5 h post delivery; cells are viewed perpendicular to the *Z*-axis. Scale bar = 100 μm.

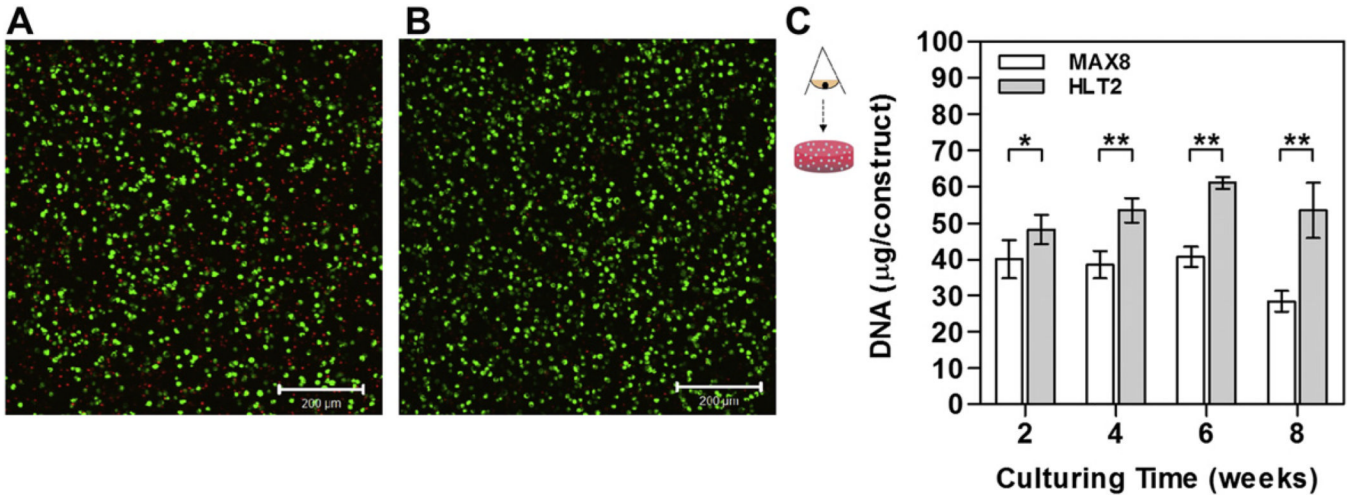

Fig. 2.

Live-dead cell viability assay of encapsulated chondrocytes in 0.5 wt% (A) MAX8 or (B) HTL2 at 24 h after syringe delivery. Cells were viewed along the z-axis. Scale bar = 200 μm. (C) Quantitative analysis of DNA content for MAX8 and HLT2 gel-cell constructs as a function of time. Error bars represent the standard deviation of 3–6 constructs. Statistical differences were assessed by a two-tailed unpaired *t*-test; # = not-significant, *$p < 0.05$, **$p < 0.01$.

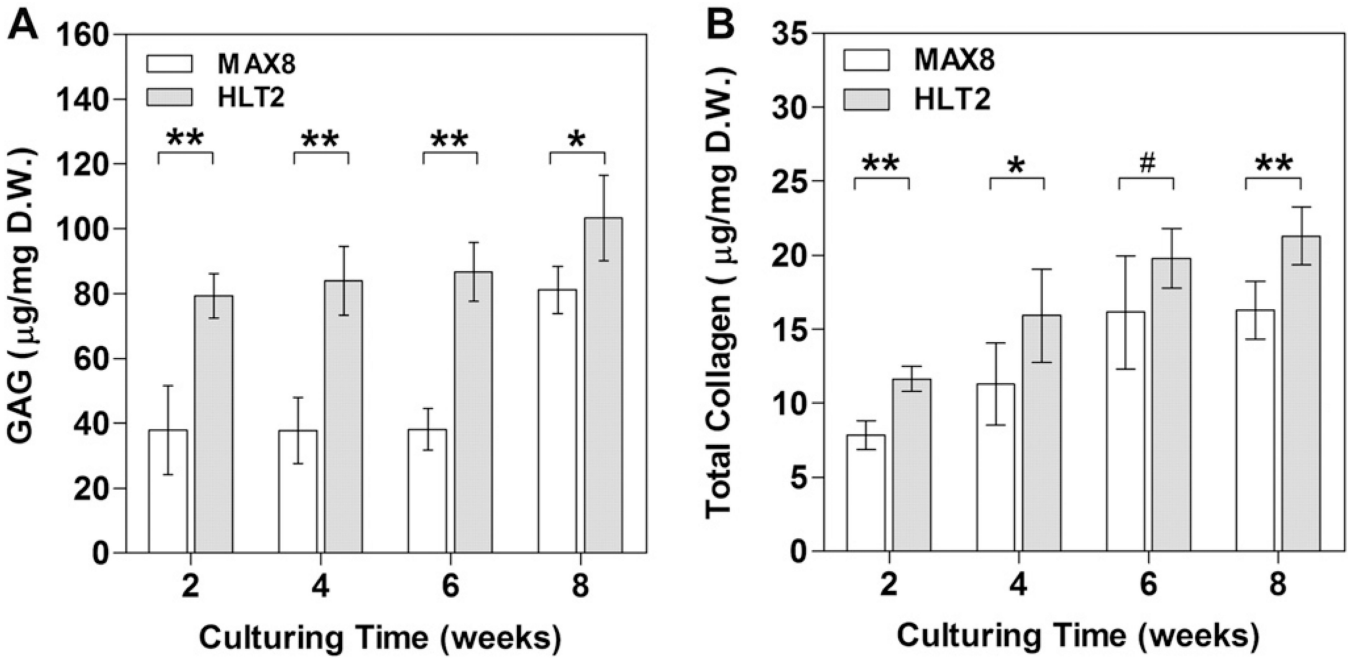

Fig. 3.

Quantitative analysis of (A) glycosaminoglycan content and (B) total collagen content for MAX8 and HLT2 gel-cell constructs as a function of time normalized to construct dry weight. Error bars represent the standard deviation of 3–6 constructs. Statistical differences were assessed by a two-tailed unpaired *t*-test; # = not-significant, *$p < 0.05$, **$p < 0.01$.

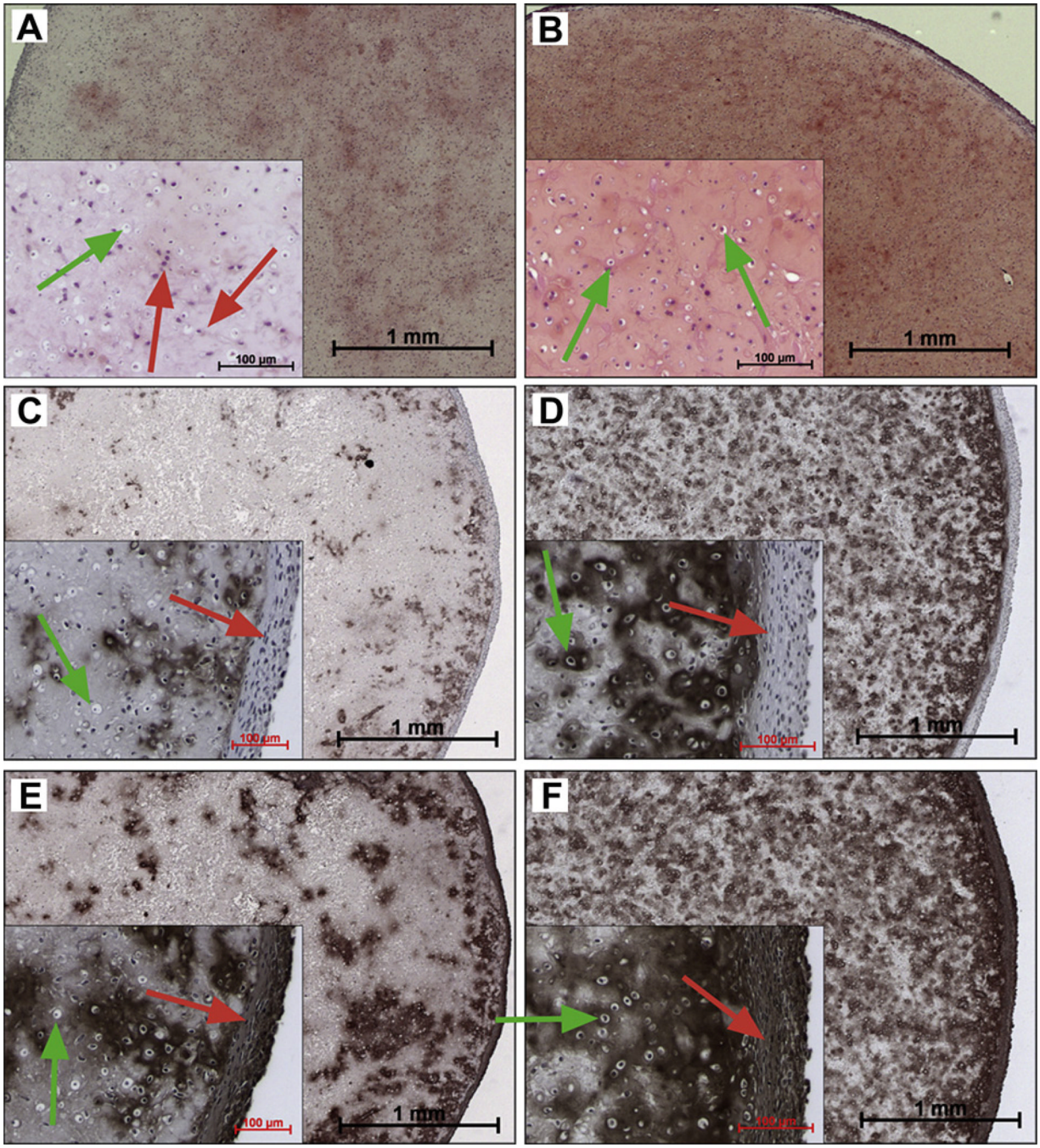

Fig. 4.

Histological assessment of 8-week MAX8 gel-cell constructs (A, C, E) and HLT2 gel-cell constructs (B, D, F). Panels A and B show GAG accumulation (red, safranin-O). Panels C and D show type II collagen accumulation (brown, IHC). Panels E and F shown type I collagen accumulation (brown, IHC). Insets represent magnified areas highlighting cell morphology (green arrows = round chonrocytic cells, red arrows = fibroblastic-like cells). Cell nuclei are stained purple/blue (hematoxylin). Scale bar = 1 mm, inset scale bar = 100 µm. (For interpretation of the references to colour in this figure legend, the reader is referred to the web version of this article.)

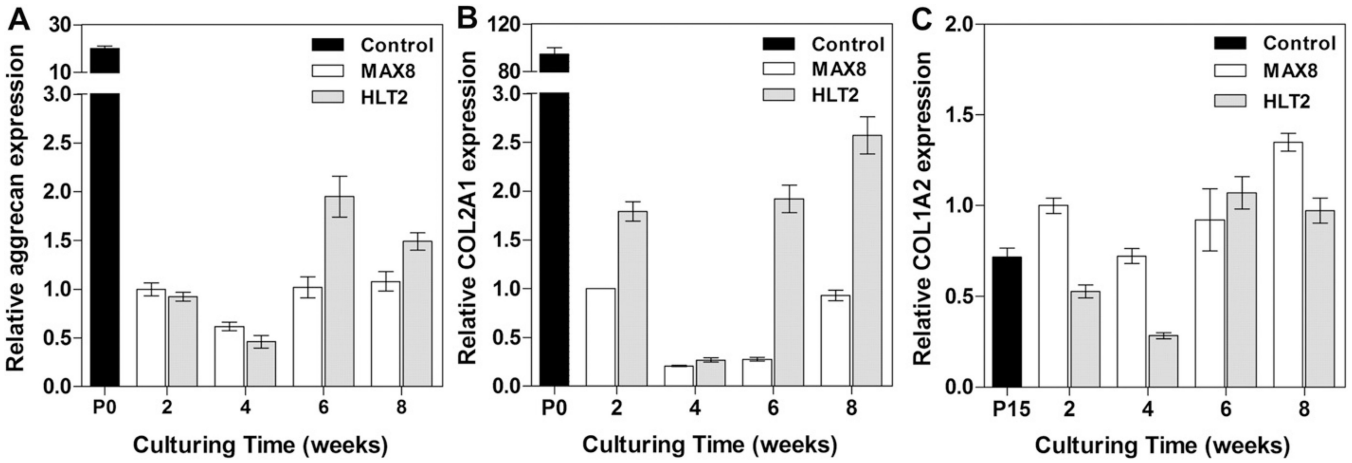

Fig. 5.

Relative gene expression of extracellular matrix proteins; (A) aggrecan, (B) type II collagen and (C) type I collagen. Gene expression levels were first normalized to the housekeeping gene, 18s ribosomal RNA and plotted relative to protein expression levels in MAX8 hydrogels at 2 weeks. RNA extracted from freshly isolated primary chondrocytes (P0) or chondrocytes at passage 15 (P15) served as controls.

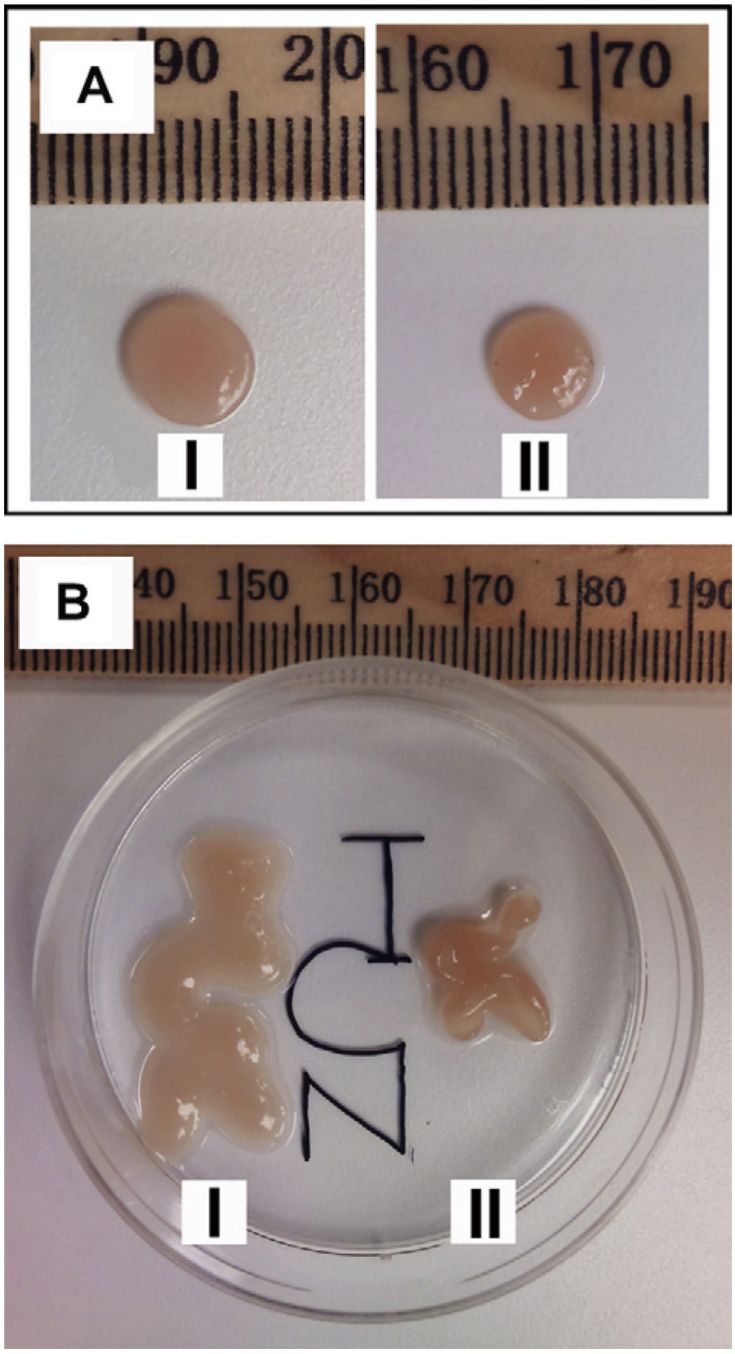

Fig. 6.

Macroscopic chondrocyte/hydrogel constructs at 8 weeks. (A) Circular constructs formed by initially delivering gels to confined cell culture inserts by syringe; (I) HLT2 and (II) MAX8. (B) Assessment of non-confined constructs to maintain their shape after syringe delivery and culturing.

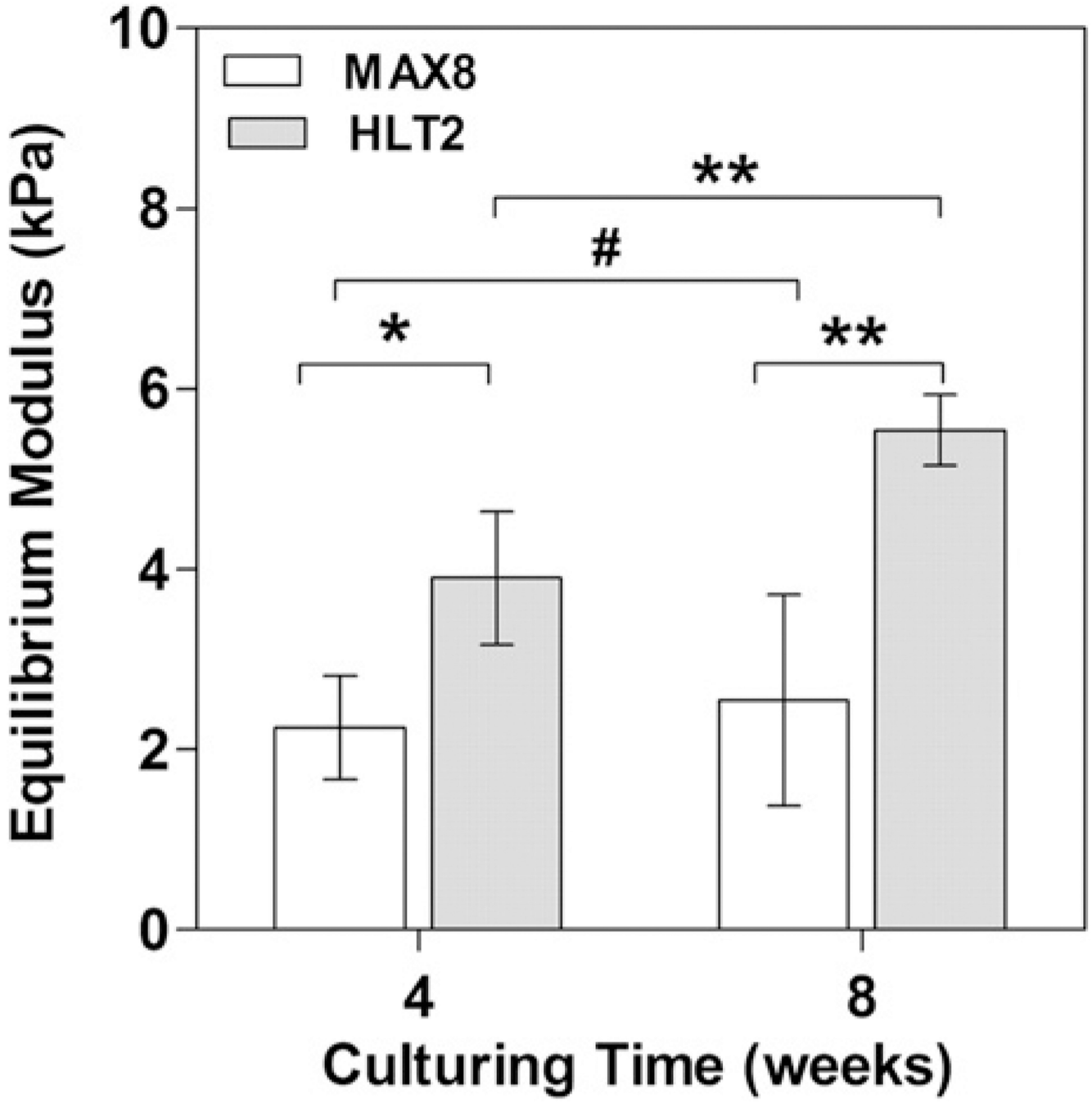

Fig. 7.

Equilibrium moduli of MAX8 and HLT2 gel-cell constructs at 4 and 8 weeks. Error bars represent standard deviation of 4 constructs. Statistical differences were assessed by a two-tailed unpaired *t*-test; # = not-significant, *$p < 0.05$, **$p < 0.01$.

Table 1

Peptide sequences and respective formal charges at pH 7.4. Schematic of hairpin with associated amino acid positions. Bold positions are on the hydrophobic face of the hairpin. Non-bold positions are on the hydrophilic face.

Peptides	Sequences	Net charge
MAX8	VKVKVKVKV ^{D}P^{L}PTKVEVKVKV-NH_2	+7
K4E	VKVEVKVKV ^{D}P^{L}PTKVEVKVKV-NH_2	+5
HIT1	VITKVKVKV ^{D}P^{L}PTKVEVKVIV-NH_2	+5
HIT2	VITKVKTKV ^{D}P^{L}PTKVEVKVIV-NH_2	+5
HLT2	VLTKVKTKV ^{D}P^{L}PTKVEVKVLV-NH_2	+5